

A New Limit on Time-Reversal Violation in Beta Decay

H.P. Mumm,^{1,2} T.E. Chupp,³ R.L. Cooper,³ K.P. Coulter,³ S.J. Freedman,⁴ B.K. Fujikawa,⁴ A. García,^{2,5}
G.L. Jones,⁶ J.S. Nico,¹ A.K. Thompson,¹ C.A. Trull,⁷ J.F. Wilkerson,^{8,2} and F.E. Wietfeldt⁷

¹National Institute of Standards and Technology, Gaithersburg, MD 20899

²CENPA and Physics Department, University of Washington, Seattle, WA 98195

³Physics Department, University of Michigan, Ann Arbor, MI, 48104

⁴Physics Department, University of California at Berkeley and Lawrence Berkeley National Laboratory, Berkeley, CA 94720

⁵Department of Physics, University of Notre Dame, Notre Dame, IN 46556

⁶Physics Department, Hamilton College, Clinton, NY 13323

⁷Physics Department, Tulane University, New Orleans, LA 70118

⁸Department of Physics and Astronomy, University of North Carolina, Chapel Hill, NC 27599

(Dated: January 19, 2013)

We report the results of an improved determination of the triple correlation $D\mathbf{P} \cdot (\mathbf{p}_e \times \mathbf{p}_\nu)$ that can be used to limit possible time-reversal invariance in the beta decay of polarized neutrons and constrain extensions to the Standard Model. Our result is $D = (-0.96 \pm 1.89(stat) \pm 1.01(sys)) \times 10^{-4}$. The corresponding phase between g_A and g_V is $\phi_{AV} = 180.013^\circ \pm 0.028^\circ$ (68% confidence level). This result represents the most sensitive measurement of D in nuclear beta decay.

PACS numbers: 24.80.1y, 11.30.Er, 12.15.Ji, 13.30.Ce

The existence of charge-parity (CP) symmetry violation in nature is particularly important in that it is necessary to explain the preponderance of matter over antimatter in the universe [1]. Thus far, CP violation has been observed only in the K and B meson systems [2–4] and can be entirely accounted for by a phase in the Cabbibo-Kobayashi-Maskawa matrix in the electroweak Lagrangian. This phase is insufficient to account for the known baryon asymmetry in the context of Big Bang cosmology [5], so there is good reason to search for CP violation in other systems. As CP and time-reversal (T) violation can be related to each other through the CPT theorem, experimental limits on electric dipole moments and T-odd observables in nuclear beta decay place strict constraints on some, but not all, possible sources of new CP violation.

The decay probability distribution for neutron beta decay, dW , can be written in terms of the beam polarization \mathbf{P} and the momenta (energies) of the electron \mathbf{p}_e (E_e) and antineutrino \mathbf{p}_ν (E_ν) as [6]

$$dW \propto 1 + a \frac{\mathbf{p}_e \cdot \mathbf{p}_\nu}{E_e E_\nu} + b \frac{m_e}{E_e} + \mathbf{P} \cdot \left(A \frac{\mathbf{p}_e}{E_e} + B \frac{\mathbf{p}_\nu}{E_\nu} + D \frac{\mathbf{p}_e \times \mathbf{p}_\nu}{E_e E_\nu} \right). \quad (1)$$

A contribution of the parity-even triple correlation $D\mathbf{P} \cdot (\mathbf{p}_e \times \mathbf{p}_\nu)$ above the level of calculable final-state interactions (FSI) implies T-violation. The PDG average of recent measurements is $D = (-4 \pm 6) \times 10^{-4}$ [7–9], while the FSI for the neutron are $\sim 10^{-5}$ [10, 11]. Complementary limits can be set on other T-violating correlations, and recently a limit on R has been published [12]. Various theoretical models that extend the SM, such as left-right symmetric theories, leptoquarks, and certain exotic fermions could give rise to observable effects that

are as large as the present experimental limits [13]. Calculations performed within the Minimal Supersymmetric Model, however, predict $D \lesssim 10^{-7}$ [14].

In the neutron rest frame, the triple correlation can be expressed as $D\mathbf{P} \cdot (\mathbf{p}_p \times \mathbf{p}_e)$, where \mathbf{p}_p is the proton momentum. Thus one can extract D from the spin dependence of proton-electron coincidences in the decay of cold polarized neutrons. Our measurement was carried out at the National Institute of Standards and Technology Center for Neutron Research [15]. The detector, shown schematically in Fig. 1, consisted of an octagonal array of four electron-detection planes and four proton-detection planes concentric with a longitudinally polarized beam. The beam, with a neutron capture fluence rate at the detector of $1.7 \times 10^8 \text{ cm}^{-2} \text{ s}^{-1}$, was defined using a series of ^6LiF apertures and polarized to $> 91\%$ (95% C.L.) by a double-sided bender-type supermirror [15]. A $560 \mu\text{T}$ guide field maintained the polarization direction throughout the fiducial volume and a current-sheet spin-flipper was used to reverse the neutron spin direction every 10 s. The symmetric octagonal geometry was chosen to maximize sensitivity to D while approximately canceling systematic effects stemming from detector efficiency variations or coupling to the spin correlations A and B [8, 16]. Each of the four proton segments consisted of a 2×8 array of silicon surface-barrier detectors (SBDs) with an active layer $300 \text{ mm}^2 \times 300 \mu\text{m}$. Each SBD was contained within an acceleration and focusing cell consisting of a 94% transmitting grounded wire-mesh box through which the recoil protons entered. Each SBD, situated within a field-shaping cylindrical tube, was held at a fixed voltage in the range -25 kV to -32 kV . The sensitive regions of the beta detectors were plastic scintillator measuring 50 cm by 8.4 cm by 0.64 cm thick, with photomultiplier tube (PMT) readout at both ends. This

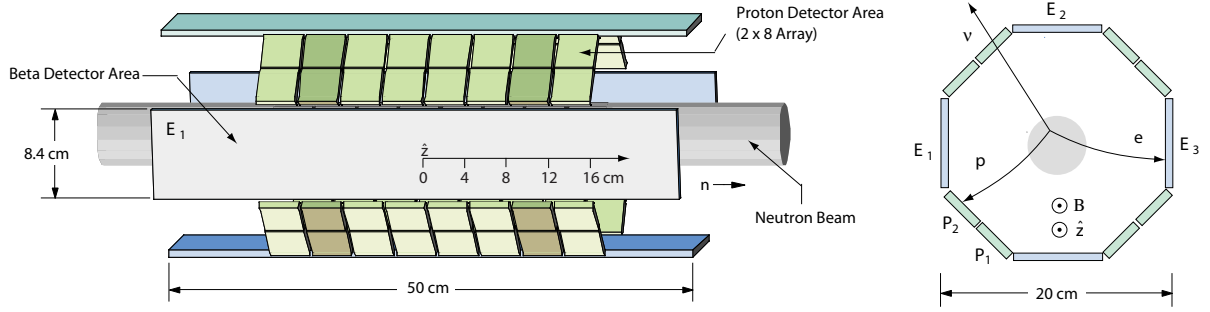


FIG. 1: A schematic of the emiT detector illustrating the alternating electron and proton detector segments. The darker shaded proton detectors indicate the the paired-ring at $z = \pm 10$ cm. The cross section view illustrates, in an exaggerated manner, the effect of the magnetic field on the particle trajectories and average opening angle. A P_2E_3 coincidence event is shown.

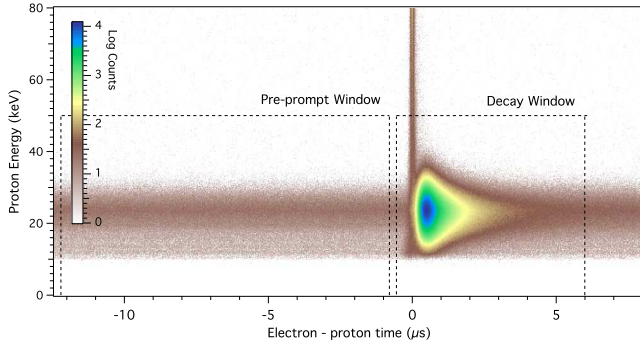


FIG. 2: Intensity log plot of SBD-scintillator coincidence data showing proton energy vs delay time. Events near $\Delta t = 0$ are prompt coincidences due primarily to beam-related backgrounds.

thickness is sufficient to stop electrons at the decay endpoint energy of 782 keV. The proton and beta detectors were periodically calibrated *in situ* with gamma and beta sources respectively. Details of the apparatus are presented elsewhere [8, 15, 17].

Data were acquired in a series of runs from October 2002 through December 2003. Typical count rates were 3 s^{-1} and 100 s^{-1} for single proton and beta detectors, respectively, while the coincidence rate for the entire array was typically 25 s^{-1} . Of the raw events, 12% were eliminated by filtering on various operational parameters (e.g. coil currents) and by requiring equal counting time in each spin-flip state. A beta-energy software threshold of 90 keV eliminated detection efficiency drifts due to changes in PMT gain coupled with the hardware threshold. This was the largest single cut, eliminating 14% of the raw events. A requirement that a single beta be detected in coincidence with each proton eliminated 7% of events. All cuts were varied to test for systematic effects.

The remaining coincidence events were divided into two timing windows: a preprompt window from $-12.3\text{ }\mu\text{s}$ to $-0.75\text{ }\mu\text{s}$ that was used to determine the background

from random coincidences, and the decay window from $-0.5\text{ }\mu\text{s}$ to $6.0\text{ }\mu\text{s}$ as shown in Fig. 2. The recoil proton has an endpoint of 750 eV. On average it is delayed by $\sim 0.5\text{ }\mu\text{s}$. The average signal-to-background ratio was $\sim 30/1$. The energy-loss spectrum produced by minimum ionizing particles in $300\text{ }\mu\text{m}$ of silicon is peaked at approximately 100 keV and, being well separated from the proton energy spectrum, yielded an estimated contamination below 0.1%. The final data set consisted of approximately 300 million accepted coincidence events.

A detailed Monte Carlo simulation was used to estimate a number of systematic effects. The program PENELOPE [18], which has been tested against data in a variety of circumstances of relevance to neutron decay [19], was embedded within a custom tracking code. All surfaces visible to decay particles were included. The Monte Carlo was based on the measured beam distribution upstream and downstream of the fiducial volume [15] and incorporated the magnetic field and electron energy threshold. A separate Monte Carlo based on the package SIMION [20], incorporating the detailed geometry of the proton cells, was used to model the proton detection response function.

Achieving the desired sensitivity to D in the presence of the much larger spin-asymmetries due to A and B depends critically on the measurement symmetry. To the extent that this symmetry is broken, corrections must be applied to the measured result. These corrections are listed in Table I and are discussed below. To extract D , coincident events were first combined into approximately efficiency-independent asymmetries

$$w^{p_i e_j} = \frac{N_+^{p_i e_j} - N_-^{p_i e_j}}{N_+^{p_i e_j} + N_-^{p_i e_j}}, \quad (2)$$

where $N_+^{p_i e_j}$ is the integrated number of coincident events in proton detector $i = 1..64$, beta detector $j = 1..4$, with neutron spin $+$ ($-$) aligned (anti-aligned) with the guide field. For uniform polarization, \mathbf{P} , the asymmetries, $w^{p_i e_j}$, can be written in terms of decay correlations as

$$w^{p_i e_j} \approx \mathbf{P} \cdot (A\tilde{\mathbf{K}}_A^{p_i e_j} + B\tilde{\mathbf{K}}_B^{p_i e_j} + D\tilde{\mathbf{K}}_D^{p_i e_j}), \quad (3)$$

where the \mathbf{K} 's are obtained from Eqn. 1 by integrating the normalized kinematic terms over the phase space of the decay, the neutron beam volume, and the acceptance of the indicated detectors [8]. $\tilde{\mathbf{K}}_A \propto \langle \mathbf{p}_e/E_e \rangle$ and $\tilde{\mathbf{K}}_B \propto \langle \mathbf{p}_\nu/E_\nu \rangle$ are primarily transverse to the detector axis but have roughly equal longitudinal components for coincidence events involving the two beta detectors opposite from the indicated proton detector (E_2 and E_3 for P_2 as shown in Fig. 1). The $\tilde{\mathbf{K}}_D$'s, however, are primarily along the detector axis and are opposite in sign for the two beta detectors. Thus for each proton detector we can choose an appropriate combination of detector pairs that is sensitive to the D -correlation but that largely cancels the parity-violating A and B correlations. One such combination is

$$v^{p_i} = \frac{1}{2}(w^{p_i e_R} - w^{p_i e_L}), \quad (4)$$

where e_R and e_L label the electron-detector at approximately 135° giving a positive and negative cross-product $\mathbf{p}_p \times \mathbf{p}_e$ respectively (P_2E_3 vs P_2E_2 as shown in Fig. 1). Proton cells at the detector ends accept decays with larger longitudinal components of $\tilde{\mathbf{K}}_A$ and are more sensitive to a range of effects that break the detector symmetry. We therefore define \bar{v} as the average of the values of v from the sixteen proton-cells at the same $|z|$, i.e. $z = \pm 2, \pm 6, \pm 10$, and ± 14 cm. Each set of detectors corresponds to a paired-ring with the same symmetry as the full detector, e.g. the shaded detectors in Fig. 1. We then define

$$\tilde{D} = \frac{\bar{v}}{P\bar{K}_D}, \quad (5)$$

where $\bar{K}_D = 0.378$ is the average of $\hat{z} \cdot (\tilde{\mathbf{K}}_D^{p_i e_R} - \tilde{\mathbf{K}}_D^{p_i e_L})$ determined by Monte Carlo. The experiment provides four independent measurements corresponding to each of the four paired-rings. The systematic corrections to \tilde{D} presented in Table I yield our final value for D . Eqn. 5 is based on the following: 1) accurate background corrections, 2) uniform proton and electron detection efficiencies, 3) cylindrical symmetry of the neutron beam and polarization, and 4) accurate determination of \bar{K}_D , P , and spin state.

Backgrounds not properly accounted for contribute two systematic errors: 1) multiplicative errors due to dilution of the asymmetries, and 2) spin-dependent backgrounds that can lead to a false D . Errors in background subtraction, as well as possible spin-dependent asymmetries in this background, have a small effect. The multiplicative correction to the value of $w^{p_i e_j}$ due to backscattered electrons was determined using the Monte Carlo.

TABLE I: Systematic corrections and combined standard uncertainties (68% confidence level). Values should be multiplied by 10^{-4} .

| Source | Correction | Uncertainty |
|-----------------------------------|----------------|--------------------|
| Background asymmetry | 0 ^a | 0.30 |
| Background subtraction | 0.03 | 0.003 |
| Electron backscattering | 0.11 | 0.03 |
| Proton backscattering | 0 ^a | 0.03 |
| Beta threshold | 0.04 | 0.10 |
| Proton threshold | -0.29 | 0.41 |
| Beam expansion, magnetic field | -1.50 | 0.40 |
| Polarization non-uniformity | 0 ^a | 0.10 |
| ATP - misalignment | -0.07 | 0.72 |
| ATP - Twist | 0 ^a | 0.24 |
| Spin-correlated flux ^b | 0 ^a | 3×10^{-6} |
| Spin-correlated pol. | 0 ^a | 5×10^{-4} |
| Polarization ^c | | 0.04 ^d |
| \bar{K}_D ^c | | 0.05 |
| Total systematic corrections | -1.68 | 1.01 |

^a Zero indicates no correction applied. ^b Includes spin-flip time, cycle asymmetry, and flux variation. ^c Included in the definition of \tilde{D} . ^d Assumed polarization uncertainty of 0.05.

The uncertainty given in Table I reflects the 20% uncertainty assigned to the backscattering fractions due to limitations of the detector and beam model and due to limited knowledge of backscattering at energies below a few hundred keV. Proton backscattering, though observable, produces a negligible effect on \tilde{D} .

In principle, the values of $w^{p_i e_j}$ are independent of the absolute efficiencies of the proton and electron detectors; however, they do depend on any energy dependence of the efficiencies through the factors $\langle \mathbf{p}_e/E_e \rangle$. Spatial variation of the efficiencies breaks the symmetry assumed in combining proton-cell data into paired-rings. Beta energy thresholds were observed to vary less than 20 keV across the detector, implying the almost negligible correction given in Table I. Proton detector efficiency variations, however, were more significant. Lower energy proton thresholds varied across the detector and over the course of the experiment. These thresholds combined with the spin-dependence of the accelerated proton energy spectra can result in significant deviations in the values of $w^{p_i e_j}$, though the effect on the value of v^{p_i} is largely mitigated because the low-energy portion of the proton energy spectrum is roughly the same for the e_R and e_L coincidence pairs. To estimate the proton-threshold-nonuniformity effect on \tilde{D} , spin-dependent proton energy spectra were generated by Monte Carlo for all proton-detector-electron-detector pairings and convoluted with model detector response functions based on fits to the average proton-SBD spectra. The average fit parameters were varied over a range characteristic of the observed variations during the run. Representative thresholds were then applied to determine the effect on

Science Foundation (PHY-0555432, PHY-0855694, PHY-0555474, and PHY-0855310).

-
- [1] A. Sakharov, Sov. Phys. Usp. **34**, 417 (1991).
 - [2] J. H. Christenson *et al.*, Phys. Rev. Lett. **13**, 138 (1964).
 - [3] B. Aubert *et al.*, Phys. Rev. Lett. **87**, 091801 (2001).
 - [4] K. Abe *et al.*, Phys. Rev. Lett. **87**, 091802 (2001).
 - [5] A. Riotto and M. Trodden, Ann. Rev. Nucl. Part. Sci. **49**, 35 (1999).
 - [6] J. Jackson, S. Treiman, and H. Wyld, Phys. Rev. **106**, 517 (1957).
 - [7] K. Nakamura *et al.*, J. Phys. G **37**, 075021 (2010), (Particle Data Group).
 - [8] L. J. Lising *et al.*, Phys. Rev. C **62**, 055501 (2000).
 - [9] T. Soldner *et al.*, Phys. Lett. B **581**, 49 (2004).
 - [10] C. G. Callan and S. B. Treiman, Phys. Rev. **162**, 1494 (1967).
 - [11] S. Ando, J. McGovern, and T. Sato, Phys. Lett. B **677**, 109 (2009).
 - [12] A. Kozela *et al.*, Phys. Rev. Lett. **102**, 172301 (2009).
 - [13] P. Herczeg, in *Proc. of the 6th Int. PASCOS-98*, edited by P. Nath (World Scientific, Singapore, 1998).
 - [14] M. Drees and M. Rauch, Eur. Phys. J. C **29**, 573 (2003).
 - [15] H. P. Mumm *et al.*, Rev. Sci. Instrum. **75**, 5343 (2004).
 - [16] E. G. Wasserman, Ph.D. thesis, Harvard University, 1994.
 - [17] H. P. Mumm, Ph.D. thesis, University of Washington, 2004.
 - [18] J. Sempau *et al.*, Nucl. Instrum. Meth. B **132**, 377 (1997).
 - [19] J. Martin *et al.*, Phys. Rev. C **73**, 015501 (2006).
 - [20] D. A. Dahl, Int. J. Mass Spectrom. **200**, 3 (2000).
 - [21] F. Calaprice, in *Hyperfine Interactions* (Springer, Netherlands, 1985), Vol. 22.